Modeling Chemotactic Cell Sorting during *Dictyostelium discoideum* Mound Formation

Bakhtier Vasiev and Cornelis J. Weijer
Department of Anatomy and Physiology, Wellcome Trust Building, University of Dundee, Dundee, United Kingdom

ABSTRACT Coordinated cell movement is a major mechanism of the multicellular development of most organisms. The multicellular morphogenesis of the slime mould *Dictyostelium discoideum,* from single cells into a multicellular fruiting body, results from differential chemotactic cell movement. During aggregation cells differentiate into prestalk and prespore cells that will form the stalk and spores in the fruiting body. These cell types arise in a salt and pepper pattern after what the prestalk cells chemotactically sort out to form a tip. The tip functions as an organizer because it directs the further development. It has been difficult to get a satisfactory formal description of the movement behavior of cells in tissues. Based on our experiments, we consider the aggregate as a drop of a viscous fluid and show that this consideration is very well suited to mathematically describe the motion of cells in the tissue. We show that the transformation of a hemispherical mound into an elongated slug can result from the coordinated chemotactic cell movement in response to scroll waves of the chemoattractant cAMP. The model calculations furthermore show that cell sorting can result from differences in chemotactic cell movement and cAMP relay kinetics between the two cell types. During this process, the faster moving and stronger signaling cells collect on the top of the mound to form a tip. The mound then extends into an elongated slug just as observed in experiments. The model is able to describe cell movement patterns in the complex multicellular morphogenesis of *Dictyostelium* rather well and we expect that this approach may be useful in the modeling of tissue transformations in other systems.

INTRODUCTION

Dictyostelium morphogenesis is initiated by aggregation of free-living single amoebae into multicellular aggregates (mounds) (Loomis, 1982; Chen et al., 1996; Firtel, 1995). The cells aggregate by chemotaxis to cAMP waves, which are initiated by the aggregation center and propagate outward as concentric or spiral waves. In the mound, the initially homogenous cell population starts to differentiate into a few types of prestalk cells and prespore cells. Differentiation of prestalk and prespore cells occurs in random positions in the mound (Takeuchi, 1991; Williams, 1995). However, in time some of the prestalk cells accumulate at the top of the mound and form a tip, while the prespore cells occupy the rest of the mound. The mound elongates under the control of the tip, and after a transient period the hemispherical mound transforms into the cylindrical slug, which falls down on the substrate and starts to migrate (Loomis, 1982). Under the influence of the right environmental signals, the slug transforms into a fruiting body consisting of stalk and spore cells. The stalk cells are dead and vacuolated while the spores survive and await favorable conditions to germinate and release single amoebae again.

This paper focuses on the modeling of cell sorting in the mound. It is known that both, prestalk and prespore cells, move in rotational fashion around the mounds vertical axis so that they form a vortex of cell flows (Siegert and Weijer, 1995; Siegert et al., 1994; Rietdorf et al., 1996; Eliott et al., 1993). The magnitude of cell velocity in these flows changes periodically and seems to be in response to counter rotating optical density waves (Rietdorf et al., 1996). Although there is as yet no direct evidences for the existence of the cAMP waves in the mound, it is clear that all mounds are organized by a variety of spiral optical density waves and that mound stage cells can respond chemotactically to cAMP (Rietdorf et al., 1996). The most natural way to explain the cell movement patterns in the mound is to assume that the cells move chemotactically in response to a scroll-shaped cAMP wave rotating in the mound. Mathematical models describing mound formation also show that transformation of the two-dimensional aggregation field into the three-dimensional mound leads to a transformation of a spiral cAMP wave to a scroll wave with the formation of corresponding vortex of cell flows rotating around the vertical axis of the mound (Bretschneider et al., 1997; Vasiev et al., 1997). After a period of rotation, the cells start to sort out. The mechanisms responsible for cell sorting in the mound are the subject of the present study.

There have been a number of mathematical models describing different stages of *Dictyostelium* development. It has been shown that the aggregation of single cells and stream formation are driven mainly by chemotaxis to propagating cAMP waves, whereas mechanical interactions of cells are not very important (Vasieva et al., 1995; van Oss et al., 1996). Models aimed to describe mound formation and slug motion show that mechanical interactions between cells are as important as chemotaxis for these phenomena (Savill and Hogeweg, 1997). These interactions can be described in a hydrodynamic way, i.e., when the mound is considered to be a drop of liquid, the cells as fluids, and

Received for publication 21 May 1998 and in final form 29 October 1998.
Address reprint requests to Dr. Cornelis J. Weijer, Department of Anatomy and Physiology, Wellcome Trust Building, University of Dundee, Dundee, DD1 5EH, UK. Tel.: 01382-345191; Fax: 0044-1382-345386; E-mail: c.j.weijer@dundee.ac.uk.

0006-3495/99/02/595/11 $2.00

their motion as a flow, which is initiated by chemotactic forces and affected by pressure and viscosity. This approach has been used by Odell and Bonner to describe slug migration (Odell and Bonner, 1986) and by (Vasiev et al., 1997) to model mound formation. Despite many differences in treatment of the details of the chemotactic signaling and movement, these two models are basically similar because both assume the liquid nature of slime mould tissue.

In this study we use a hydrodynamic approach to model cell sorting in the mound. We consider the mound as consisting of two mixed liquids corresponding to the two cell types, prestalk and prespore cells. Both liquids are chemotactically reacting with rotational movement to a counter rotating scroll wave of cAMP in the mound. We investigate which differences in the properties of these liquids can result in their separation, i.e., in cell sorting. Contrary to many other models of cell sorting, which consider differential adhesion as the driving force for cell sorting (Umeda, 1989, 1993; Savill and Hogeweg, 1997), we focus on differential chemotaxis and differential excitability. We show that sorting of prestalk cells to the top of the mound (while the prespore cells occupy the rest of its volume) takes place when the excitability of prestalk cells and their chemotactic movement is higher than that of prespore cells. Another important question, which we address in our model, is what mechanism is responsible for the transformation of the shape of the mound. We show that scroll waves of cAMP rotating around the vertical axis of the mound lead to cell flows that result in transformation of a hemispherical mound into a cylinder. Therefore, the shape of the cAMP wave (i.e., scroll) in the mound determines the formation of a cylindrical slug.

MODEL

The basic assumptions of the model are the following.

1. **The mound is a three-dimensional structure with free boundaries.** The shape of the mound changes gradually over time. The mound forms by aggregation of single cells, which initially form a flat layer on the substrate but during aggregation pile on top of each other to form a hemispherical aggregate. The mound transforms in a tall cylindrical-shaped-standing slug.
2. **The mound is an excitable medium.** There is strong experimental evidence for the existence of chemical waves of cAMP. These waves are generated by the cells, propagate through the mound, and synchronize the movement of the cells. To model these waves, we consider the mound to be an excitable medium.
3. **The mound is an incompressible viscous liquid.** The main experimental evidence suggesting that the mound behaves as a viscous liquid comes from the analysis of the cell movement patterns in the mound. These movement patterns show strong similarity to the laminar flows observed in a liquid. While single cells (at the early aggregation) exhibit a distinct pulsatile motion, i.e., directed motion during the rising phase of the passing cAMP waves and random motion at all other times, cells in the mound move continuously despite the periodic nature of chemotactic signal (Rietdorf et al., 1996; Siegert and Weijer, 1995; Rietdorf et al., 1997). The cells do not slow down significantly between chemotactic waves, i.e., they move more or less continuously. At the same time, the cells do not strictly keep their neighbors. This implies that there exist strong interactions between cells, i.e., the cells make and break contacts continuously. Furthermore, cells in mounds, which rotate around a central core, show a velocity profile that is smooth in space. The velocity is maximal in the middle between the center of the mound and the periphery (Siegert et al., 1994; Siegert and Weijer, 1995). These properties are similar to those of a viscous liquid. On the cellular level, this behavior is presumably based on the shape flexibility of the individual cells. They change their shape during movement and in response to interactions with other cells.
4. **The mound is composed of two kinds of fluids.** These fluids correspond to prestalk (20–25% of the total amount of cells) and prespore cells. These cell types differ in many properties but here we only take into account differences in their chemotactic response and signaling systems. Based on experimental data we assume that prestalk cells are faster and more excitable compared with prespore cells. It has been shown that aggregation-stage cells can be separated into populations that are going to become prestalk and prespore cells and that the cells that are going to become prestalk show higher frequency optical density oscillations as the cells that will become prespore (Weijer et al., 1984). It was shown that purified populations of prestalk and prespore cells exhibit excitable cAMP kinetics and that prestalk cells are more excitable (Otte et al., 1986). It was shown that isolated prestalk cells move faster in response to a chemotactic cAMP signal when put on an agar substrate compared with similarly treated prespore cells (Mee et al., 1986; Early et al., 1995). This suggests strongly that prestalk cells can develop a stronger chemotactic movement force than prespore cells.

Before we introduce the model equations, we want to state that the goal of this study is to understand the mechanisms of cell sorting and to give a qualitative rather than a quantitative description of the process. A good quantitative description of cell sorting is still impossible because of a lack of detailed knowledge of the signaling system and the mechanical properties of the cells and their interaction with the substrate. For example, to model the cAMP waves we use equations that do not reflect any details of the real cell-signaling system. The model parameters are chosen such that a correct relationship between experimentally measurable data such as velocity of cells and waves exists. However, our results are robust and qualitatively insensitive to reasonable variations of the model parameters.

To model propagation of cAMP waves in a mound, we use the FitzHugh-Nagumo equations, which are widely known as describing a prototype excitable medium:

$$\partial g/\partial t = D\Delta g - k_g(g - g_0)(g - g_1)(g - g_2) - k_r r \quad (1)$$

$$\partial r/\partial t = (g - g_0 - r)/\tau \quad (2)$$

Here g is assumed to define the level of extracellular cAMP, and r is the proportion of active and inactive cAMP receptors (Martiel and Goldbeter, 1987) or activated α subunits of the inhibitory G-proteins (Tang and Othmer, 1994, 1995). D is the diffusion coefficient for cAMP; τ is a time scaling factor for the variables r and g. k_g and k_r define the rate of cAMP production and hydrolysis respectively. Although the Eqs. 1 and 2 are not as good as Martiel-Goldbeter (Martiel and Goldbeter, 1987) or Tang-Othmer models (Tang and Othmer, 1994) in describing the details of the *Dictyostelium* signal relay system, they can be integrated much faster (allowing to use larger time and space steps), and therefore are better suited for the time consuming calculations presented here.

Cell movement is described as a flow in incompressible liquid by the Navier-Stokes equation:

$$\rho(\partial \mathbf{V}/\partial t + (\mathbf{V}\nabla)\mathbf{V}) = \mathbf{F}_{ch}\eta\Delta\mathbf{V} - \nabla p \quad (3)$$

The left-hand side of the equation describes the acceleration of the fluids under the influence of the forces given in the right-hand side of the equation. $\mathbf{V}$ is a velocity of the flow; ρ is a density of the liquid, $\mathbf{F}_{ch}$ is the chemotactic force per volume. The second term on the right-hand side of Eq. 3 describes cell-cell friction: η is the viscosity coefficient. The last term on the right-hand side defines the forces caused by the pressure, p, which develops in the mound as a result of the chemotactic cell movement.

We assume that the chemotactic force is proportional to the gradient of cAMP:

$$\mathbf{F}_{ch} = K_{ch}(\partial g/\partial t)\nabla g \quad (4)$$

in which K_{ch} is equal to zero when $\partial g/\partial t \leq 0$, and to a positive constant when $\partial g/\partial t > 0$. The cAMP time derivative is used to distinguish the wave front, where cells accelerate in response to the chemotactic signal, from the wave back, where cells are desensitized and do not respond to the cAMP gradient. Eq. 4 cannot be considered to be an exact description of chemotaxis, however, it takes into account the most important features: accumulation of kinetic energy and impulse of motion along the cAMP gradient. How cells accelerate in reality is unknown. Using Eq. 4 we assume that accelerating cells get traction from surrounding cells and the extracellular matrix, whose own acceleration is neglected.

Moving cells slow down for two reasons: 1) because of viscous interactions between cells given by second term in the right-hand side of Eq. 4. These interactions are very strong in the mound, as cells instantly form and break contacts with each other and with the extracellular matrix. As a result of viscous interactions, cells tend to have the same velocity, an averaged velocity of all cells in the mound. 2) Another force slowing down the cells derives from friction to the sheath of the mound. The mechanical properties of the sheath are not known very well, but one can assume that the sheath is moving only to a very limited extent or not at all. The friction between the moving cells and the stationary sheath slows down not only cells located in the immediate vicinity of the sheath, but also all other cells in the mound because of the viscous cell-cell interactions.

The last term in the right hand side of Eq. 4 is a force generated by a pressure field in the mound. This force is responsible for the mound's incompressibility and allows cells to reorient the direction of their motion so that they not necessarily move toward the source of chemotactic signal. Pressure results in the occurrence of upward cell flows, which cause the transformation of a two-dimensional collection of cells into a hemispherical mound (Vasiev et al., 1997) and the further transformation of the mound into a slug (present study).

To model cell sorting in the mound, we assume that the mound is heterogeneous, i.e., it consists of two kinds of fluids, which correspond to prestalk and prespore cells, each characterized by the volume fractions, α_1 and α_2:

$$\begin{aligned} &\alpha_1 + \alpha_2 = 1 \text{ inside the mound;} \\ &\alpha_1 + \alpha_2 = 0 \text{ outside the mound.} \end{aligned} \quad (5)$$

To model difference in excitability of prestalk and prespore cells we assume that they differ in their rate of cAMP production:

$$k_g = k_1\alpha_1 + k_2\alpha_2 \quad (6)$$

in which k_1 and k_2 define the rate of cAMP production by each cell type. In the same way (making other parameters in Eqs. 1 and 2 cell-type dependent), we can model other kinds of differences in the cAMP relay systems of prestalk and prespore cells.

Similar to the differential excitability, we model differential chemotactic movement by introducing parameters, K_1 and K_2, which define the chemotactic force developed by prestalk and prespore cells:

$$K_{ch} = K_1\alpha_1 + K_2\alpha_2 \quad (7)$$

Consequently the velocities of prestalk, V_1, and prespore, V_2, cells will be different and can be found using the momentum balance equation for each subliquid:

$$\begin{aligned} &\rho\, d(\alpha_i\mathbf{V}_i)/dt \\ &\quad = \mathbf{F}_i + \eta\nabla(\alpha_i\nabla\mathbf{V}_i) - \alpha_i\nabla p + (-1)^i\Psi\alpha_1\alpha_2(\mathbf{V}_1 - \mathbf{V}_2) \end{aligned} \quad (8)$$

in which the index i = 1,2 denotes prestalk or prespore cells, $\mathbf{F}_i$ corresponds to chemotactic forces as they result from Eq. 7, the effects of viscosity and pressure are proportional to their volume fractions, and the last term defines the viscous interaction between the two liquids. Volume frac-

tions for prestalk and prespore cells are found using the equation for the conservation of mass:

$$\partial\alpha_i/\partial t = \nabla(\alpha_i \mathbf{V}_i) \quad \text{in which i} = 1,2. \tag{9}$$

To stabilize the numerical integration of Eqs. 8 and 9 we used staggered grids and have simplified Eq. 8 to:

$$\rho\,\alpha_i(\partial \mathbf{V}_i/\partial t + (\mathbf{V}_i\nabla)\mathbf{V}_i = \mathbf{F}_i + \eta\alpha_i\Delta\mathbf{V}_i - \alpha_i\nabla p + (-1)^i\Psi\alpha_1\alpha_2(\mathbf{V}_1 - \mathbf{V}_2) \tag{10}$$

Using Eq. 10 instead of Eq. 8 we neglected two terms: one containing the spatial derivative of the volume fractions, $\eta\nabla\alpha_i\nabla\mathbf{V}_i$, which results from the viscous term and causes the most severe numerical problems, and a term $(\mathbf{V}\alpha_i\nabla\mathbf{V}_i)$, which derives from the left-hand side of Eq. 8. Initial computations have shown that adding the last term does not significantly affect the velocity and sorting patterns described below. That probably indicates that terms containing the divergence of velocity are small and that the term $\eta\nabla\alpha_i\nabla\mathbf{V}_i$ which we removed from the right-hand side of the equations also would not alter obtained results. In addition, to accelerate the computations, we neglect the viscous interactions between prestalk and prespore cells ($\Psi = 0$). As we have checked in computations with nonzero Ψ, these interactions do not effect the way of sorting but increase a total time required for it, because they result in a decrease of the difference in velocities between prestalk and prespore cells.

All calculations were performed in three-dimensional domains using finite difference equations. Eqs. 1 and 2 were integrated by the Euler explicit method using the forward time centered space method for the diffusion term (Press et al., 1988). Eq. 3 was integrated by the two-step projection method (Kothe et al., 1991) using upwind methods for the convection term and a simultaneous over-relaxation scheme (SOR) for the pressure Poisson equation (PPE) (Press et al., 1988). Eqs. 9 and 10 were integrated explicitly, using the upwind method for the convection terms and taking the value for pressure, *p,* from the solution of Eq. 3. These methods are stable with the space and time steps used ($h_x = 0.6$; $h_t = 0.06$) and the following choice of parameters, a diffusion coefficient in Eq. 1 of $D = 1$, viscosity in Eq. 3 ($\eta = 1$), and the observed maximal value of chemotactic flow ($\max|\mathbf{V}|<1.$ in all computations).

For the cAMP concentration field (Eq. 1) and volume fraction fields (Eq. 9) we used Neumann's no-flux boundary conditions at the boundary of the medium as well as at the free boundary of the mound. For the velocity fields (3,8) we checked both Neumann and Dirichlet (zero value) boundary conditions on the free boundary of the mound and used no-slip conditions on the boundaries of the medium. To check an influence of diffusive cAMP flows from the mound to the substrate (see Fig. 7 *A*) we modified the boundary condition at the bottom boundary of the medium in the following way. 1) We assumed that there is a stationary level of cAMP in the substrate far from the mound, g_∞. 2) We assumed that the difference between a cAMP level (g_{in}) in grids at bottom plane of the mound (our 1st plane) and that (g_{out}) at upper plane of the substrate (bottom boundary of our computational medium) is a fixed part of a difference: $g_{in} - g_{out} = \alpha(g_{in} - g_\infty)$. This expression was used to find a cAMP level at the bottom boundary of the computational medium: $g_{out} = g_{in} - \alpha(g_{in} - g_\infty)$. This allowed us to save computational time by avoiding direct computations of the cAMP flows into the substrate.

The location of the free surface was detected by tracking massless particles distributed in the volume of the mound (MAC method (Harlow and Welch, 1965)). Initially the particles were located in the exact middle of number of grids, forming a hemispherical structure in three-dimensional space. At each time step, the particles were shifted according to the velocity of the fluid flow (given by Eq. 3) in the occupied grids. Tracking of the particles allowed detecting the changes in the shape and location of the mound in the following manner. We assumed that all the grids, which are occupied by particles or located one grid apart from those occupied by particles, constitute the mound. All other grids represent the outer space. The cAMP concentrations and the cell velocities were computed in all grids considered to be part of the mound. The boundary conditions were applied to those grids contacting outer space. Using this definition of the mound we were able to track the changes in the mound's shape and location during the simulations.

The computations were performed in media of $70 \times 70 \times 50$ grids (Figs. 1 and 2, and see Fig. 7), $50 \times 50 \times 40$ (Fig. 3), and $60 \times 60 \times 100$ (see Fig. 6) with the initial diameter of mound varying between 24 and 36 space units. Model parameters were $g_0 = 0.3$; $g_1 = 0.35$; $g_2 = 1.3$; $\tau = 4$; $k_r = 1.5$; $D = 1$; $\rho = 1$; $\eta = 1$; k_g varied between 5.4 and 6.0; K_{ch} varied between 1 and 4. Program was written using Microsoft Visual C++4 and run on Pentium-Pro200 PC. Time, required for single computation, varied from 10 to 100 hours. For example, the computation presented in Fig. 1 (10,000 time steps each including about 100 iterations of PPE solver) took 58 hours.

The velocity of the cAMP waves measured in our model was 1.2 space units per time unit, the period of scroll wave rotation varied between 20 and 50 time units. The velocity of the fluid flows inside the mound varied between 0.2 and 0.8 space units per time unit (depending on K_{ch}). Assuming that a time unit is equal to 0.1 min and the space unit is equal to 5 μm, these parameters result in a mounds size of up to 200 μm, a period for cAMP wave rotation of 2–5 min, a velocity of the cAMP waves of $\sim$60 μm/min, and a velocity of the cell flows of 10–40 μm/min. All these numbers are close to those measured in experimental conditions (Siegert et al., 1994; Rietdorf et al., 1996).

RESULTS

Cell sorting in the mound

To study cell sorting, we have performed computations starting with a hemispherical mound consisting of two cell

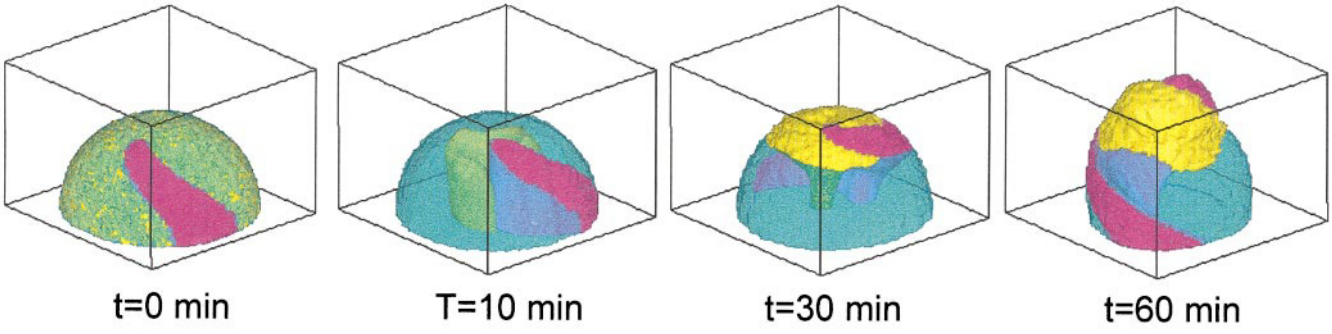

FIGURE 1 Cell sorting in the mound. The mound consists of 20% of prestalk cells (*yellow*) and 80% prespore cells (*blue*). The cell types differ in chemotactic velocity ($K_1 = 2$ and $K_2 = 1$ in Eq. 6) and in excitability ($k_1 = 6.0$ and $k_2 = 5.4$ in Eq. 1). Initially the mound is a hemisphere in which a cAMP scroll wave (*purple*) is initiated and rotates clockwise, and both cell types mixed randomly. Affected by the cAMP waves, the cells move and sort so that the prestalk cells collect at the top of the mound and form a tip.

types that are initially randomly distributed. We have found that the conditions under which the cells sort out in the way which is in best agreement with experimental observations is when the cell types differ both in velocity and excitability in such a way that faster cells are more excitable. An example of cell sorting using these conditions is shown in Fig. 1. A scroll wave of cAMP rotating in a hemispherical mound causes cell movement in the mound. The movement patterns (flows) are different for the different cell types and lead to a redistribution of the cells in the mound. Initially, the faster cells collect in the middle of the mound along its vertical axis and then they start to move up and form a plume-like pattern with most of the fast cells on top. These cells will form a tip. Because of the accumulation of the more excitable cells on the top and the less excitable cells in the body of the mound, the scroll wave of cAMP becomes twisted. In addition to its clock-wise rotation it gets a downward component that leads to further accumulation of the fast moving cells on top and elongation of the mound upwards. During this process the period of the scroll wave decreases from 48 to 21 time units (or from 4.8 to 2.1 min according to our scaling).

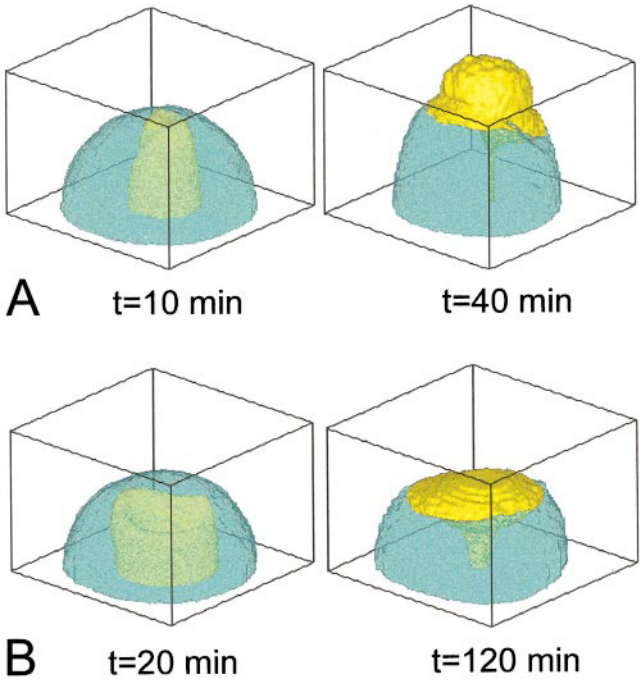

FIGURE 2 Cell sorting in the mound. Conditions the same as in Fig. 1 except that the prestalk and prespore cells do not differ in their excitability. The excitability is high ($k_1 = k_2 = 6.0$) in (*A*) and low ($k_1 = k_2 = 5.4$) in (*B*). At the early stages of sorting, there is a qualitative difference in the sorting pattern observed in both cases: the faster cells form a ring in (*A*) or collect directly in the middle of the mound in (*B*). At the later stages of sorting, this qualitative difference reduces to a more quantitative one: the faster cells form, in both cases, plume-like structures that differ in the sizes of their cross section in their bottom and top parts. For clarity of cell sorting patterns, cAMP waves are not shown.

We also checked the cell sorting when the cell types differ only in excitability or only in velocity. We have found that there is no cell sorting if cell types differ only in their excitability. The mound in this case is similar to a uniform mound in which the excitability is average of those of both cell types. If cell types differ only in their velocity of chemotactic motion, they do sort out. But the sorting pattern obtained is rather different from that shown in Fig. 1. In this case, cell-sorting stops at the stage when faster cells form a plume-like structure surrounded by slower cells. Two cases of sorting from differences in chemotactic velocity are shown for mounds of different excitability (Fig. 2). In a highly excitable mound, the faster cells almost immediately form a plume-like pattern that in time becomes thinner at the base and wider at the top. In a less excitable medium the faster cells initially form a ring-shaped structure at the bottom of the mound. In time, the ring contracts and elongates upward and finally transforms also into a plume-like structure but with a wider base as in a highly excitable medium.

Shape transformations in mounds consisting of one cell type

In this section we investigate the properties of uniform mounds consisting only of one cell type. We hope that further insight obtained in these studies will help us to

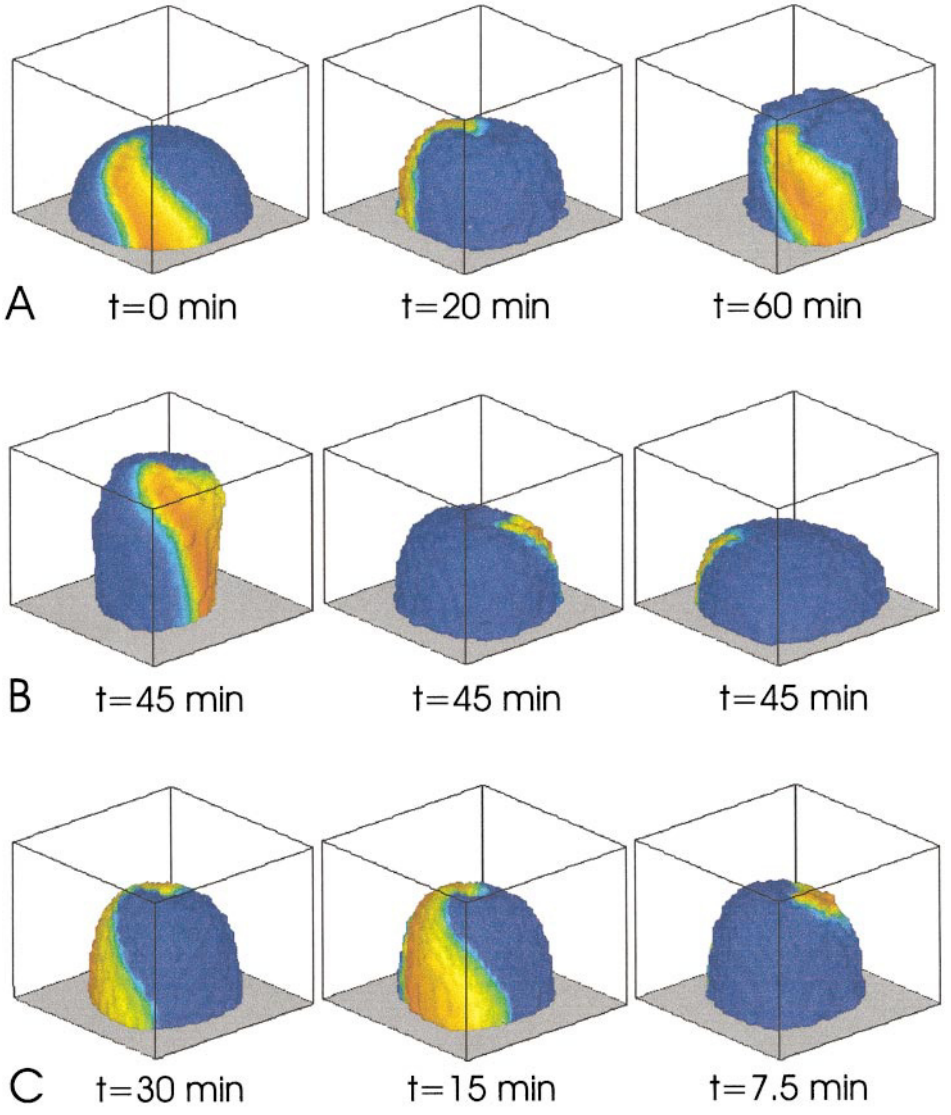

FIGURE 3 Transformations of uniform hemispherical mounds. (*A*) Hemispherical mound transforms to a cylinder (k_g = 5.7, K_{ch} = 2). (*B*) Radius of cylinder depends on its excitability. Three mounds of different excitability are shown. k_g = 6.0, 5.7, and 5.4, respectively. The periods of the cAMP scroll rotations are 19, 32, and 54, respectively, for these mounds. K_{ch} = 2 in all cases shown. The rate of the shape transformation of a mound is proportional to velocity of the motion of its cell. Shown are three mounds of the same excitability (k_g = 6.0) but with different velocities of cell motion (K_{ch} = 1, 2, and 4, respectively). In this figure, the cAMP isoconcentrations are mapped on the mounds surface. Blue represents low cAMP, red high cAMP.

understand the results of the simulations shown in Figs. 1 and 2. We want to understand why cells sort out, why faster cells collect on the top of the mound, and why they form a tip. The question we address at the moment is what is the stationary shape of a uniform mound and how is it influenced by the choice of model parameters. Beginning with a hemispherical mound where cAMP scroll wave has been initiated, we found the following. 1) The mound always tends to evolve to a cylindrical shape (Fig. 3 *A*). The transition period is very long (at least a few tens of cAMP wave rotations) and increases with a decrease in velocity of chemotactic motion or with an increase in a mounds volume. 2) The radius of the cylinder decreases as the excitability of the mound increases (Fig. 3 *B*). As a result more excitable mounds form more elongated cylinders. 3) There seems to exist proportionality between the velocity of chemotactic motion and the rate of the shape transformation (Fig. 3 *C*). The velocity does not appear to have a large influence on the final stationary shape of the mound.

The mound shown in Fig. 3 *A* changes its shape from hemispherical to cylindrical. The final cylindrical shape is stable. The mounds shown in Fig. 3 *B* have different excitabilities. Their shapes are all investigated after a fixed time (t = 45 min) starting from the same initial hemispherical shape. Although these mounds have not yet achieved their stationary shape, it can be easily recognized that they tend to go towards cylindrical shapes and that the radius of these cylinders increases gradually as mound's excitability decreases. The mounds in Fig. 3 *B* have very similar shapes. They have evolved from the same initial condition and differ only in their cell's chemotactic movement response. The time of observation multiplied by the chemotactic forcing is constant for all the mounds shown. It shows that the transformation rate of the mound shape is proportional to the chemotactic movement response.

Mechanisms of mound shape transformations

The shape transforms result from cell flows, which occur in response to rotating cAMP waves. The velocity field for the cell flows in a uniform mound is shown in Fig. 4 *A*. The cell

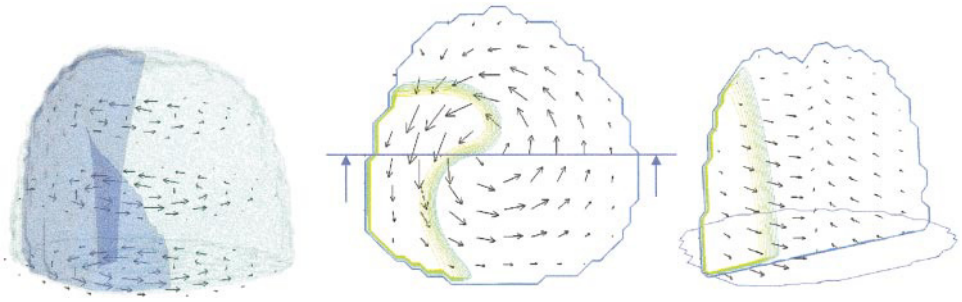

FIGURE 4 Velocity field in mound. The velocity field in the volume, the horizontal bottom plane, and the vertical cross-section of the mound are shown for the second mound in Fig. 3 *C*. The mound is drawn transparent to show the scroll wave of cAMP rotating inside (also drawn transparent), and arrows indicate magnitude and direction of velocity. Maximal size of arrows corresponds to velocities ~20 μm/min. The cAMP wave in the cross-section is shown by its isolines. The vertical cross-section (taken at the position indicated by the line in the middle figure) of the mound is slightly rotated to visualize the cell flows orthogonal to this section. In the left-hand side of the section, the flow (*arrows*) is towards the observer, whereas in the right-side, the flow is directed away from the observer.

flows form a vortex, which rotates in direction opposite to the direction of rotation of the cAMP scroll wave. From a horizontal section of the velocity field (Fig. 4 *B*), it can be seen that the cells move tangentially around the tip of the spiral, which results from a cross-section of the filament of the cAMP scroll wave. It is also seen that the velocity of cell movement is modulated by the cAMP wave. Cells accelerate in the front of the cAMP wave and then gradually slow down until they accelerate again in response to the next wave. A vertical cross-section of the velocity field (Fig. 4 *C*) shows that there is an upward flow of the cells in the middle of the mound near the filament of the cAMP scroll wave. This flow is responsible for the transformation of the shape of the mound. The force responsible for the vertical flows is a hydraulic pressure generated by the moving cells. The pressure develops because the chemotactic force developed by the accelerating cells is not really tangential; it has an inward component for cells located at the periphery of mound and an outward component for the cells inside the spiral core. These inward-outward components occur because the cAMP wave is scroll shaped. If the number of cells forced inward is higher than the number of cells forced outward, the hydraulic pressure increases in the core of scroll, which forces the cells in the core to move upward (because they cannot move downward). This flow leads to elongation of the mound and therefore to a decrease in diameter of its base. As the mound becomes thinner, the number of cells tending to move inward decreases. When it becomes approximately equal to the number of cells moving outward, the hydrodynamic pressure in the scroll core falls, and the vertical flow comes to a halt. Thus, the shape of the mound stabilizes when the radius of the horizontal cross-sections of the mound achieves a critical value, i.e., the mound attains a cylindrical shape. This critical value is defined by a condition in which the inward chemotactic forcing on the periphery of the mound is balanced by outward chemotactic forcing in the middle of the mound so that there are no vertical flows inside the mounds anymore. Finally, the radius of the stationary cylinder depends on the shape of the cAMP wave, i.e., it depends on the excitability of the mound.

Mechanisms of cell sorting

The same mechanisms, which are responsible for changing the shape of the uniform mound, lead also to cell sorting in a heterogeneous mound. Cells in the periphery of the mound tend to move inward, i.e., there is a competition for the space in the middle of the mound (the scroll's core) between cells of different type. Faster cells, which are able to move more effectively, chemotactically win this competition and accumulate in the middle of the mound (Fig. 1 *B*). Because in the middle of the mound there is an upward flow, most of the faster cells move further up and finally form a plume-like structure pointing to the top surrounded by slower cells. If the difference between the cell types is only confined to the velocity of motion, cell sorting stops at this stage (Fig. 2). If the cell types differ, in addition, in excitability, the structure formed by high excitable cells deforms the shape of the scroll wave. The plume-like structure formed by prestalk cells results in an anisotropy in the mound, i.e., the top of the mound becomes more excitable than its bottom. As a result, the scroll wave becomes twisted and gets new downward component causing further upward cell flows in the mound (Fig. 5). All cells try to move up, but again the faster cells win the competition for the space on the top of the mound (compare velocity profiles for prestalk and prespore cells in vertical cross section given in Fig. 5). Finally, all the faster cells collect at the top of the mound and form a tip (Fig. 1). The radius of the tip is smaller than the radius of the mound. Because of the sorting of the more excitable cells in the tip, the tip can now support a spiral with a smaller core resulting in a smaller tip diameter (see Fig. 3 *B*).

Transformation of a mound to a slug

The shape of the mound shown in Fig. 1 changes over the time accompanying the cell sorting. The mound elongates in time and soon reaches the upper boundary of the medium. To investigate the evolution of the mound further, we have prolonged the computations in a medium of modified size (Fig. 6). We have found that the mound, undisturbed by medium boundaries, continues to elongate and, finally de-

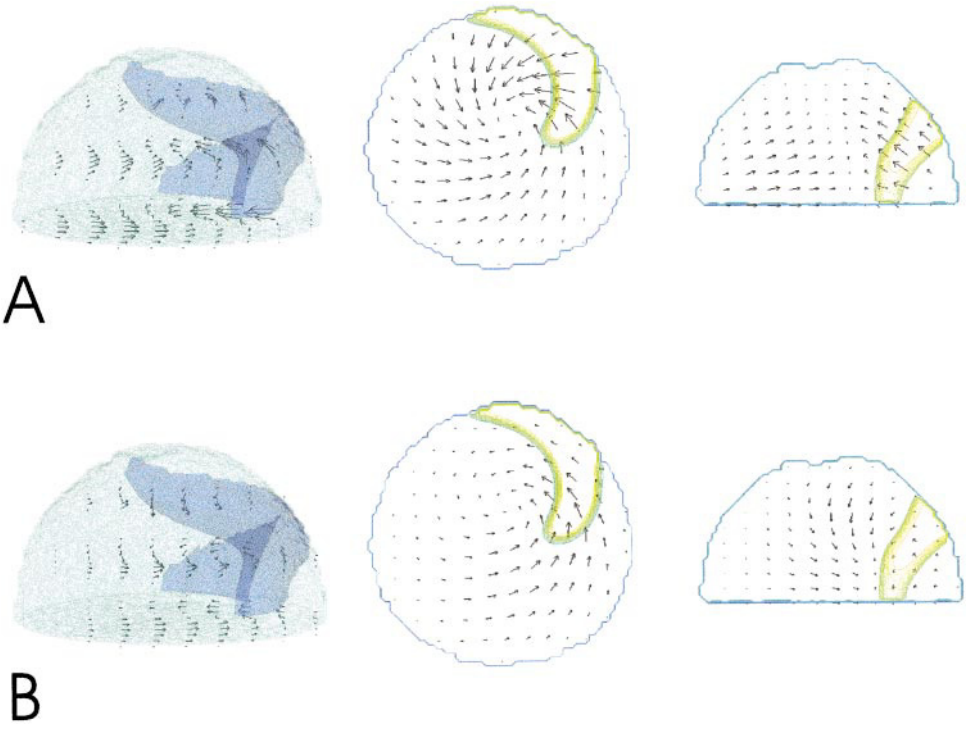

FIGURE 5 The velocity field and its cross sections for prestalk (*A*) and prespore (*B*) cells in the mound shown in Fig. 1 at $t = 30$ min. The velocity fields are shown in the same way as in Fig. 4.

velops into a slug. Investigation of the velocity fields of the cells in this structure shows that cells in the tip move more in a rotational fashion, while cells in the tail make a more upward directed motion very much in agreement with the patterns of cell movement observed in slugs (Siegert and Weijer, 1992; Abe et al., 1994; Dormann et al., 1996). The final structure shown in Fig. 6 is not stable. It tends to fall down (at least comes into contact with one of the side boundaries of the medium) as observed under experimental conditions. This structure then should start to move, which is something we are still checking in further simulations.

Effect of leaking of cAMP from mound to the substrate on the sorting process

Under normal laboratory conditions the mound sits on the substrate, normally an agar surface. There is a cAMP (diffusive) flow from mound to the substrate. This flow introduces cAMP gradients in the lower part of the mound, which possibly can effect the cell sorting. We have checked this in our model by allowing a cAMP flow to occur over the mound's bottom boundary (boundary condition for the cAMP field at the bottom boundary of the computational medium were modified as described in the model section). The resulting sorting patterns are shown in Fig. 7 *A*. A comparison with Fig. 1 shows that there is a stronger upward flow of prestalk cells, so that they begin to collect at the top of mound instead of collecting in the middle first to form of a plume-like pattern. Altogether, sorting is accelerated and takes less time. We explain these changes in sorting in the following way: the diffusion of cAMP from the mound to substrate creates a vertical cAMP gradient in the very bottom of the mound (in our calculations the cAMP

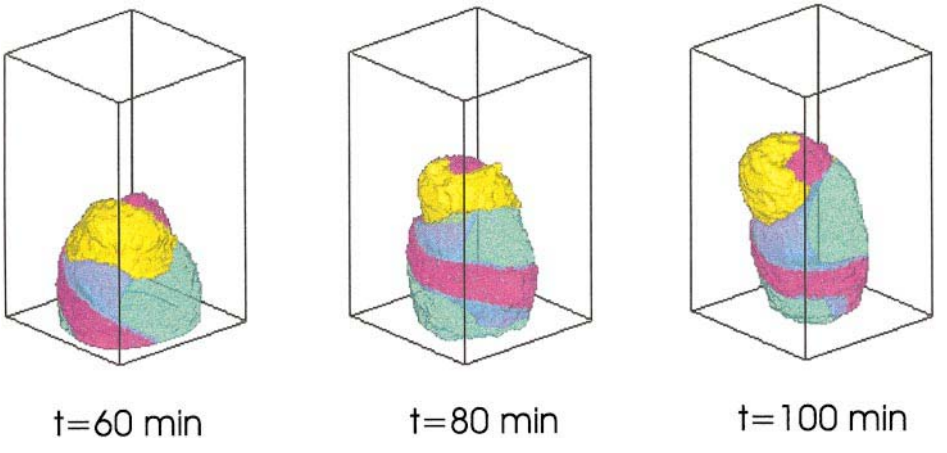

FIGURE 6 Transformation of a mound into a slug. The mound shown in Fig. 1 has been placed in larger medium ($60 \times 60 \times 100$ grids) and allowed to evolve further. It transforms from a mound to a standing slug.

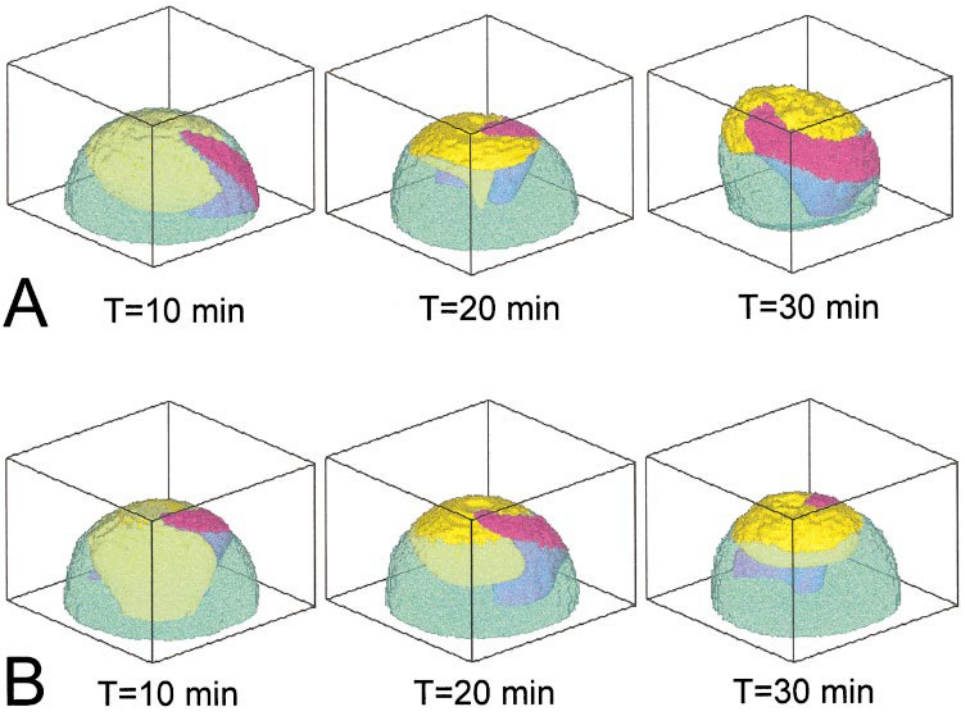

FIGURE 7 Effect of cAMP diffusive flow from the mound into the substrate (*A*) and the effect of the oxygen (diffusing from the surface into the mound) on excitability (*B*) on the cell-sorting process. All conditions are the same as in Fig. 1 with the following exceptions: (*A*) the boundary condition for the cAMP field at the mound substrate interface is not Neumann (no flux) but: $g_{out} = g_{in} - \alpha(g_{in} - g_\infty)$ in which $\alpha = 0.9$ and $g_\infty = 0$. (*B*) Oxygen diffuses into the mound from the free surface and is consumed everywhere inside ($D_O = 1$ and $k_O = 0.002$ in Eq. 11). As a result, the concentration of oxygen falls from 1 at the mound's surface to 0.93 at the center of the mound. The oxygen affects the rate of cAMP release by the cells according to Eq. 12. The production of cAMP by the cells (k_g in Eqs. 1 and 6) is made proportional to the oxygen concentration. To restore an average excitability in the mound, we slightly increased (compared with all previous computations) the values of k_1 and k_2: $k_1 = 6.2$ and $k_2 = 5.6$.

gradients extend only 3–4 planes up (15–20 μm) into the mound). This gradient forces prestalk cells to move up from the bottom. As a result of this motion, the mound becomes inhomogeneous, excitability decreases in the bottom. This inhomogeneity adds to the vertical gradients of cAMP and, what is more important, results in cAMP gradients further up in the mound. Now even more prestalk cells become involved in the upward motion. In turn, sorting causes differences in the excitability at higher levels in the mound. From a certain time onwards, only the difference in excitability between the upper and lower levels in the mound forces further upward sorting. Thus, the diffusive cAMP flow from the mound to the substrate fires the sorting process in vertical direction. As soon as sorting starts, it works in an autocatalytic regime propagating itself upward through the volume of the mound.

Effect of diffusive oxygen flows into the mound on sorting process

It is known that oxygen activates many processes in cells and affects sorting pattern presumably by affecting the amount of cAMP released (Sternfeld and David, 1981a, 1981b). As oxygen diffuses from the air through mound's surface into the mound where it is used by cells, oxygen levels should fall from the surface to the inside. As a result, the mound could become inhomogeneous with respect to its excitability, and this then can affect the cell sorting process in the mound. To check this possible effect we included one more variable, *O,* into our model such that: 1) oxygen level is constant (O = 1.) outside the mound; 2) oxygen diffuses into the mound and is consumed there:

$$\partial O/\partial t = D_o \Delta O - k_o O \qquad (11)$$

and 3) the rate of cAMP production by the cells (in Eq. 6) is proportional to the oxygen level:

$$k_i = O k_i$$

in which

$$i = 1,2 \text{ indicates prestalk or prespore cells.} \qquad (12)$$

The resulting cell sorting pattern in this modification of the model is shown in Fig. 7 *B*. A comparison with Fig. 1 shows that the flow of prestalk cells towards the top of the mound is accelerated, whereas the flow to the center seems to be reduced. Again, sorting occurs faster similar to the case shown in Fig. 7 *A*. An explanation for the changes in the sorting pattern observed comes from the consideration of the excitability in the mound. The concentration of oxygen inside the mound decreases from the surface to the middle and achieves the lowest level in the exact middle at the bottom of the mound. Accordingly the excitability in the

mounds, center increases from the bottom to the top. This induces a vertical flow of prestalk cells. In each horizontal section of the mound, the excitability increases towards the periphery resulting in a reduced cell flow towards the center. All together these changes result in a faster upward movement of the prestalk cells.

DISCUSSION

The main goal of this work is to understand the mechanisms responsible for cell sorting in the mound. Our general assumption that cell sorting results from differential chemotactic cell flows inside the mound was confirmed by calculations. The calculations also showed that the characteristic shape changes of the mound from a hemisphere to an elongated cylinder, the slug, are easily accounted for by the same mechanisms. Our model describes chemotactic cell sorting, and the accompanying shape transformation remarkably well. Our explanations for these phenomena are as follows. 1) The most important factor for cell sorting is a difference in velocity of prestalk and prespore cells (in agreement with experimental data (Siegert and Weijer, 1992; Early et al., 1995)). Both cell types move in the same direction along cAMP gradients, but the faster cells accumulate at the source of cAMP waves, the spiral tip, and displace the slower prespore cells there. 2) The way of sorting is determined by the shape of the cAMP wave. The shape changes, in turn, because of sorting, as a result of the differential excitability of the sorting cells. Forced by the scroll wave of cAMP, the faster cells collect in the middle and on the top of the mound forming a plume-like structure (Fig. 2). Because the faster cells are more excitable, this sorting results in the mound becoming inhomogeneous with respect to its excitability. This in turn causes a twist of the scroll wave, which allows all faster cells to collect on the top of the mound, finally forming a distinct morphological tip (Fig. 1). 3) The transformation of the shape of the mound results from the chemotactic flows inside the mound. The precise manner of the shape transformation depends (through these flows) on the shape of cAMP wave. As we have seen, a scroll wave leads to transformation of hemispherical mound to cylindrical slug. Contrary, a pacemaker located in the middle of the bottom plane of the mound stabilizes its hemispherical shape (results are not shown).

Differences in the velocities of prestalk and prespore cells were modeled by differential chemotaxis, i.e., prestalk cells were assumed to exert stronger forces in response to the chemotactic signal than prespore cells. Another way to achieve this difference is to assume that both exert the same chemotactic force but that they differ in their adhesive properties, resulting in an effective slower movement of prespore cells. In terms of our model it could mean that cell types differ in their viscosity coefficients. Calculations in which we assumed that prestalk cells are characterized by a smaller viscosity than to prespore cells have resulted in exactly the same results as shown in Fig. 2.

The scroll wave of cAMP in the mound is stable and does not change at all when the cell types differ only in their velocity of motion (Fig. 2). An additional difference in the excitability of the cell types forces the scroll wave to change. One way for a scroll wave to change is to twist (Fig. 1). However, in some cases the scroll wave becomes unstable so that its filament changes the shape and location in the mound over the time resulting to complicated cAMP wave patterns. Such wave patterns have recently also been observed in experiments (Dormann and Weijer, unpublished observations). We have not shown images from the computations showing this behavior but want to note here that this kind of instability takes place when the filament of the cAMP scroll wave in an inhomogeneous mound begins to drift horizontally, resulting in different drift rates in different cross-sections and this therefore destroys the scroll.

There is at least one contradiction between the pattern of cell sorting seen in experiments and that shown in Fig. 1. In our calculations, the prestalk cells sort to the middle of the mound first and then move up (Fig. 1). Although cell movement of prestalk cells during sorting has not yet been observed directly in experiments, it seems from the analysis of sequenced static images that the initial salt and pepper pattern changes gradually in a pattern in which prestalk cells accumulate at the tip. The impression is that prestalk cells move up throughout the whole volume of the mound without accumulating in the center first. If this is the case, it means that something that is important for cell sorting was not taken into account in our calculations. To check this further, we performed the computations shown in Fig. 7, i.e., we took into account a cAMP flow between the mound and the substrate (Fig. 7 *A*) and effect of oxygen on an excitability of the mound (Fig. 7 *B*). The results of these computations are twofold: in both cases the rate of sorting in vertical direction increases. As a result, the cells collect quickly at the top of the mound and omit the intermediate stage where they collect along the vertical axis of the mound. This is certainly in better agreement with the experimental observations. The less desirable feature of both calculations is that tips do not form easily under both sets of assumptions. At the end of sorting process, we have a rather flat collection of cells at the top of the mound, which is not changing in time. A tip is not formed because the effective excitability at the top of the mound is not as high as it was in the case shown in Fig. 1. In Fig. 1, a tip forms because the core of the scroll wave is small on the top, formed by higher excitable prestalk cells, and large at the bottom, formed by low excitable prespore cells. However, in the calculation shown in Fig. 7 this difference is reduced because of the more random distribution of prestalk and prespore cells during the sorting process. Finally, when the prestalk cells move up, they form a wide thin cap on top of the prespore cell mass and this reduces their effective excitability (because of interaction with the prespore cells), resulting in no further contraction of the tip.

Many results of our model calculations can be checked experimentally. For example, we would expect that in mounds formed by cells (mutants) in which the cell types differ only in excitability, cell sorting would not take place. Accumulation of the faster cells in the middle of mound can be checked in synergy experiments between mutants differ-

ing only in their velocity. An example of this type of behavior was recently shown to occur in synergy experiments between wild-type cells and a cytoskeleton mutant cell line. The latter mutant (an alpha-actinin-gelation factor double null mutant) showed a significantly reduced movement speed compared with wild-type cells (Rivero et al., 1996). In synergy experiments in which a small percentage of wild-type cells were mixed with mutant cells, it was found that the wild-type cells collected first in the middle and then on top of the mounds. These results have been confirmed recently with synergy experiments between wild-type and a talin null strain, which also show sorting of the wild-type cells in the talin null mutant. (Weijer et al., in preparation).

The basic assumption used in the model presented here is that cell flows inside the mound can be considered as a fluid flows in liquid. The results of the present study can be considered as a confirmation of the validity of this assumption. The velocity fields for cell flows in the mound, shown in Figs. 4 and 5, are in good agreement with the experimental data obtained by the tracking of moving cells. In both cases, the cells move in rotational fashion in the direction opposite to that of the rotation of the scroll of cAMP. The velocity of the cells is modulated in a cross section of the mound as observed in experiments (Siegert et al., 1994): the velocity is smaller in the middle of the mound as well as at its periphery while achieving maximum speed in the region equidistant from the mound's middle and its surface. In addition, the velocity of the fluids (cells) change periodically in response to periodic chemotactic cAMP waves.

We thank Till Bretschneider for discussions. This work was supported by a grant from the BBSRC.

REFERENCES

Abe, T., A. Early, F. Siegert, C. Weijer, and J. Williams. 1994. Patterns of cell movement within the Dictyostelium slug revealed by cell type-specific, surface labeling of living cells. *Cell.* 77:687–699.

Bretschneider, T., B. Vasiev, and C. J. Weijer. 1997. A model for cell movement during Dictyostelium mound formation. *J. Theor. Biol.* 189:41.

Chen, M. Y., R. H. Insall, and P. N. Devreotes. 1996. Signaling through chemoattractant receptors in dictyostelium. *Trends Genet.* 12:52–57.

Dormann, D., F. Siegert, and C. J. Weijer. 1996. Analysis of cell movement during the culmination phase of Dictyostelium development. *Development.* 122:761–769.

Early, A., T. Abe, and J. Williams. 1995. Evidence for positional differentiation of prestalk cells and for a morphogenetic gradient in Dictyostelium. *Cell.* 83:91–99.

Eliott, S., G. H. Joss, A. Spudich, and K. L. Williams. 1993. Patterns in Dictyostelium discoideum—the role of myosin-II in the transition from the unicellular to the multicellular phase. *J. Cell Sci.* 104:457–466.

Firtel, R. A. 1995. Integration of signaling information in controlling cell-fate decisions in Dictyostelium. *Genes Dev.* 9:1427–1444.

Harlow, F. H., and J. E. Welch. 1965. Numerical calculation of time dependent viscous incompressible flow of fluid with a free surface. *Phys. Fluids.* 8:2182–2189.

Kothe, D. B., R. C. Mjolsness, and M. D. Torrey. 1991. RIPPLE: a computer program for incompressible flows with free surfaces. *Los Alamos Natl. Lab.* LA-12007-MS.

Loomis, W. F. 1982. The Development of Dictyostelium Discoideum. Ac. Press, New York.

Martiel, J.-L., and A. Goldbeter. 1987. A model based on receptor desensitization for cyclic AMP signaling in Dictyostelium cells. *Biophys. J.* 52:807–828.

Mee, J. D., D. M. Tortolo, and M. B. Coukell. 1986. Chemotaxis-associated properties of separated prestalk and prespore cells of Dictyostelium discoideum. *Biochem. Cell Biol.* 64:722–732.

Odell, G. M., and J. T. Bonner. 1986. How the Dictyostelium discoideum grex crawls. *Phil. Trans. R. Soc. Lond. B* 312:487–525.

Otte, A. P., M. J. E. Plomp, J. C. Arents, P. M. W. Janssens, and R. Van Driel. 1986. Production and turnover of cAMP signals by prestalk and prespore cells in Dictyostelium discoideum cell aggregates. *Differentiation.* 32:185–191.

Press, W. H., B. P. Flannely, S. A. Teukovsky, and W. T. Vetterling. 1988. Numerical Recipes in C. Cambridge University Press, Cambridge.

Rietdorf, J., F. Siegert, S. Dharmawardhane, R. A. Firtel, and C. J. Weijer. 1997. Analysis of cell movement and signalling during ring formation in an activated G alpha 1 mutant of Dictyostelium discoideum that is defective in prestalk zone formation. *Dev. Biol.* 181:79–90.

Rietdorf, J., F. Siegert, and C. J. Weijer. 1996. Analysis of optical-density wave-propagation and cell-movement during mound formation in Dictyostelium-discoideum. *Dev. Biol.* 177:427–438.

Rivero, F., B. Koppel, B. Peracino, S. Bozzaro, F. Siegert, C. J. Weijer, M. Schleicher, R. Albrecht, and A. A. Noegel. 1996. The role of the cortical cytoskeleton—F-actin cross-linking proteins protect against osmotic-stress, ensure cell-size, cell-shape and motility, and contribute to phagocytosis and development. *J. Cell Sci.* 109:2679–2691.

Savill, N. J., and P. Hogeweg. 1997. Modelling morphogenesis: from single cells to crawling slugs. *J. Theor. Biol.* 184:229–235.

Siegert, F., and C. J. Weijer. 1992. Three-dimensional scroll waves organize Dictyostelium slugs. *Proc. Natl. Acad. Sci. USA.* 89:6433–6437.

Siegert, F., and C. J. Weijer. 1995. Spiral and concentric waves organize multicellular Dictyostelium mounds. *Curr. Biol.* 5:937–943.

Siegert, F., C. J. Weijer, A. Nomura, and H. Miike. 1994. A gradient method for the quantitative analysis of cell movement and tissue flow and its application to the analysis of multicellular Dictyostelium development. *J. Cell Sci.* 107:97–104.

Sternfeld, J., and C. N. David. 1981a. Cell sorting during pattern formation in Dictyostelium. *Differentiation.* 20:10–21.

Sternfeld, J., and C. N. David. 1981b. Oxygen gradients cause pattern orientation in Dictyostelium cell clumps. *J. Cell Sci.* 50:9–17.

Takeuchi, I. 1991. Cell sorting and pattern formation in Dictyostelium discoideum. *In* Cell-Cell Interactions in Early Development. J. Gerhart, editor. Wiley-Liss, New York. 249–259.

Tang, Y. H., and H. G. Othmer. 1994. A G protein-based model of adaptation in Dictyostelium discoideum. *Math. Biosci.* 120:25–76.

Tang, Y. H., and H. G. Othmer. 1995. Excitation, oscillations and wave propagation in a G- protein-based model of signal transduction in Dictyostelium discoideum. *Phil. Trans. R. Soc. Lond. B.* 349:179–195.

Umeda, T. 1993. A thermodynamical model of cell distributions in the slug of cellular slime mold. *Bull. Math. Biol.* 55:451–464.

Umeda, T. A. 1989. A mathematical model for cell sorting, migration and shape in the slug stage of Dictyostelium discoideum. *Bull. Math. Biol.* 51:485–500.

van Oss, C., A. V. Panfilov, P. Hogeweg, F. Siegert, and C. J. Weijer. 1996. Spatial pattern formation during aggregation of the slime mould Dictyostelium discoideum. *J. Theor. Biol.* 181:203–13.

Vasiev, B., F. Siegert, and C. J. Weijer. 1997. A hydrodynamic model for Dictyostelium discoideum mound formation. *J. Theor. Biol.* 184:441.

Vasieva, O. O., B. N. Vasiev, V. A. Karpov, and A. N. Zaikin. 1995. Modeling of Dictyostelium discoideum aggregation. *Biofizika.* 40:393–411.

Weijer, C. J., S. A. McDonald, and A. J. Durston. 1984. A frequency difference in optical-density oscillations of early Dictyostelium discoideum density classes and its implications for development. *Differentiation.* 28:9–12.

Williams, J. 1995. Morphogenesis in Dictyostelium—new twists to a not-so-old tale. *Curr. Opin. Genet. Dev.* 5:426–431.